Frequency-dependent selection predicts patterns of radiations and biodiversity

Carlos J. Melián[1], David Alonso[2], Diego P. Vázquez[3,4], James Regetz[1] & and Stefano Allesina[1]

[1]*National Center for Ecological Analysis and Synthesis, University of California, 735 State St., Suite 300, Santa Barbara, CA 93101, USA.*

[2]*Community and Conservation Ecology Group, University of Groningen, Haren, Groningen, The Netherlands.*

[3]*Inst. Argentino de Investigaciones de las Zonas Áridas, CONICET, CC 507, AR-5500, Mendoza, Argentina.*

[4]*Instituto de Ciencias Básicas, Universidad Nacional de Cuyo, Centro Universitario, M5502MJA Mendoza, Argentina.*

Most empirical studies support a decline in speciation rates through time[1–4], although evidence for constant speciation rates also exists[5–7]. Declining rates have been explained by invoking niche-filling processes[8–12], whereas constant rates have been attributed to non-adaptive processes such as sexual selection, mutation, and dispersal[13]. Trends in speciation rate and the processes underlying it remain unclear, representing a critical information gap in understanding patterns of global diversity. Here we show that the speciation rate is driven by frequency dependent selection. We used a frequency-dependent and DNA sequence-based model of populations and genetic-distance-based speciation, in the absence of adaptation to ecological niches. We tested the frequency-dependent selection mechanism using cichlid fish[14] and Darwin's finches[15], two classic model systems for which speciation rates and richness data exist. Using negative frequency dependent selection, our model both predicts the declining speciation rate found in cichlid fish and explains their species richness. For groups like the Darwin's finches, in which speciation rates are constant and diversity is lower,

the speciation rate is better explained by a model without frequency-dependent selection. Our analysis shows that differences in diversity are driven by larger incipient species abundance (and consequent lower extinction rates) with frequency-dependent selection. These results demonstrate that mutations, genetic-distance-based speciation, sexual and frequency-dependent selection are sufficient not only for promoting rapid proliferation of new species, but also for maintaining the high diversity observed in natural systems.

Speciation is one of the most complex phenomena in nature, yet the effects of its tempo and mode for biodiversity patterns are still controversial[16]. Niche filling is considered the dominant mechanism explaining the initial explosion of diversity observed in radiations[17,18]. In contrast, speciation driven by niche-independent mechanisms such as sexual selection, physical barriers, or dispersal limitation do not predict such a temporal trend of declining speciation rates during a radiation event[14,19]. Although ecological opportunity (the availability of an unoccupied adaptive zone) can explain rates of diversification in some radiating lineages, this is not sufficient for a radiation to occur[3,20]. Instead of attributing the propensity to radiate to external influences like niche availability, an alternative hypothesis can be based in the genome properties evolved during the evolutionary history of organisms. We explore this hypothesis using two models, one with frequency-dependent selection and one without it. Both models involve DNA sequence-based evolution of populations via a process of sexual selection, mutation, and genetic-distance-based speciation, all in the absence of adaptation to ecological niches. Significantly for the results we report here, no analytical approximations of the tempo and mode of speciation incorporating sexual mating have previously been shown to explain observed patterns of radiations and diversity without invoking adaptation to ecological niches.

We simulated the evolution of a population whose members, at the beginning, have identical genomes. The population evolves under the combined influences of sexual reproduction and mutation (μ). During reproduction, potential mates are identified from those whose genomes are

sufficiently similar to that of the reproducing individual ($q^{\min}$). A mate is chosen from this set at random. An offspring is then dispersed in the environment. This minimal form of sexual selection called assortative mating[21,22] is sufficient for speciation at least when there is no genetic linkage[23]. Genetic similarity among individuals can be represented by an evolutionary graph in which nodes are individuals and edges connect reproductively compatible individuals[24] (Fig. 1). We identify a species as a group of organisms reproductively separated from all the others by genetic restriction on mating, but connected among themselves by the same condition. Thus, two individuals connected at least by one pathway through the evolutionary graph are considered conspecific, even if the two individuals themselves are reproductively incompatible.

We simulated several variants of the model. We report here the one that uses haploid and hermaphrodites individuals. Our density of individuals is one per site, and these numbers are kept constant by assuming zero-sum dynamics. Birth-death zero-sum stochastic models are equivalent to their non zero-sum counterparts at stationarity[25]. Factors influencing speciation may differ between regions of the genome, and regions of the genome involved in reproductive isolation may differ between taxa and the temporal stages of the speciation process[26]. In our model, the genome of each individual is considered effectively infinite (i.e., a very large string of nucleotides). Using zero-sum dynamics and infinite genome size allow us to approximate the tempo of speciation and also to identify the conditions for each of two alternative modes of speciation in the evolutionary graph.

At the beginning of the simulation, all individuals are reproductively compatible, corresponding to a completely connected graph. Because of mutations that can eventually reduce genetic similarity below the threshold required for mating, the graph will lose connections as generations pass (Fig. 1). The rate at which connections are lost in the evolutionary graph, and thus the tempo of speciation, depends on the mechanisms driving genome diversification. To explore the tempo of speciation and its implications for biodiversity patterns, we generated a second model with nega-

tive frequency dependent selection. Rare types have an increased chance of reproduction, whereas common types are likely–but not guaranteed–to become rare. In summary, individuals with few connections, and therefore less common alleles, have greater mating success and can spread their alleles more quickly through the population. Apart from the asymmetry introduced by the different reproductive probabilities at the individual level, these two models are identical.

With appropriate parameter values, both models can produce speciation events (i.e., sexual isolation of subpopulations in the genome space). We identified two distinct modes of speciation that can, under the right conditions, occur in the evolving graph: fission and mutation-induced speciation. Fission takes place when the death of an individual breaks a link in what was the sole genetic pathway connecting some members of a species; this gives rise to one or more new species (Fig. 1). Mutation-induced speciation happens when a newly produced offspring is disconnected from its parents. However, this latter form of speciation requires the mutation rate to exceed some minimum value ($\mu_{\min}$) necessary to satisfy the inequality $q^{kj} < q^{\min}$, where k is the offspring and j are the parents of k (Fig. 1). This minimum mutation rate is:

$$\mu_{\min} = -\left(\frac{log\left(\frac{2q^{\min}}{1+q^{\min}}\right)}{2}\right). \tag{1}$$

For example, if offspring become inviable once genetic divergence exceeds 5% (i.e., $q^{\min} = 0.95$), then the minimum mutation rate needed to achieve mutation-induced speciation is ≈ 1.3 x 10^{-2}. Because of this strict condition, fission is the only mode of speciation in the biologically relevant portion of model parameter space (Supplementary section A3).

Per capita speciation rate, defined as the total number of speciation events divided by the product of the number of generations times population size (J), can be well approximated for the model without frequency-dependent selection:

$$\nu = \alpha + \beta\left[\frac{-2\mu + log(\frac{1+\omega}{2})}{log(q^{\min})}\right]. \tag{2}$$

Fitting this expression to the speciation rates obtained via simulation yielded least-squares regression coefficient estimates of $\alpha = -0.23$ and the slope $\beta = 0.88$ ($r^2 = 0.98$, $p < 0.001$), where ω is the expected similarity between the two parents. Because the similarity is in the range [$q^{\min}$,1], assuming a uniform distribution on the similarity leads to an expected value $\omega = (1 + q^{\min})/2$. This approximation suggests that speciation rate is independent of population size (Supplementary section A3 and figure S3).

The models successfully generate changes over time in the tempo of speciation, the distribution of incipient species abundance, and both the number and diversity of contemporary species. In Figs. 2 and 3, we summarize the following two key predictions for the species number through time and species richness consistent with Darwin's finches and cichlid fish.

First, we predict whether the rate of speciation will remain constant or decline over time depending upon the addition of frequency-dependent selection. Fig. 2a shows how the number of extinct and extant species varies over time. After a transient period, during which mutation introduces genetic variability into the initially identical population, the number of species increases rapidly. The two models then diverge dramatically. In the model without frequency-dependent selection, speciation rate remains constant. This pattern is consistent with the literature on whole-tree cladistic analysis[6], the record of marine invertebrate fossils from the Phanerozoic eon[7], and (over shorter time frames) observed genetic differences among North American songbirds[5]. The number of contemporary species (Fig. 2b), diversity (Inset Fig. 2b), and the abundance of the new species (Fig. 2c) are lower than in the frequency-dependent model. In the frequency-dependent case, rapid speciation is followed by a plateau with few speciation events, consistent with molecular data for several groups showing declining speciation rates through time[3,4,27,28]. This model predicts a greater number of contemporary species, higher diversity, and a more symmetric abundance distribution of incipient species; these are all attributes of rapid radiations.

Second, frequency-dependent selection reproduces cichlid radiations in absence of niche filling and its absence generates the Darwin's finches radiation. Fig. 3a and 3b show the best fit to the data for the number of species and speciation events through time. We predict decline over time and constant speciation rate in the cichlids and Darwin's finches with and without frequency-dependent selection, respectively (data not shown). The expected distributions of species abundance derived from those predictions depart dramatically. For the $Limnochromini$ tribe, the model predicts high diversity, with most species having similar abundances (inset Fig. 3a); for the Darwin's finches, the model predicts much lower species diversity, with most species being rare (insets Fig. 3b).

Several studies have concluded that sympatric speciation only occur if a stringent set of conditions were met[9,12]. Likewise, for the models we have explored, sympatric speciation can be highly unlikely or even impossible in biologically relevant areas of parameter space (i.e., $q^{\min} < Q^* = \frac{1}{\theta+1}$, where $\theta = 4J\mu$, Supplementary information). This suggests that there are certainly cases in which environmental heterogeneity, geographical barriers and dispersal limitation, and/or range expansion must play an important role in radiations. We note, however, that those factors do not generate decay through time in speciation rate in the absence of niche filling (Supplementary figure S5). Interestingly, the absence of frequency-dependent selection does not capture the exponential growth in number of species in the last stage of Darwin's finches radiation. Time lag for extinctions[27], taxonomic splitting but also the increase in heterogeneity with time in the Galápagos archipelago (i.e., more islands, habitat diversity and food types)[15] are some of the factors that may hamper model predictions in this case. Nevertheless, the balance of results for both the cichlids and the Darwin's finches suggest that the properties of genomes have played a role in radiating lineages in the absence of geographical barriers or environmental heterogeneity.

Current biodiversity theory, from population genetics[11,13] to island biogeography and its extensions[29], explain species abundance patterns for many groups, but cannot predict the tempo and mode of speciation nor their implications for radiations and diversity patterns. As Fig. 3

illustrates, our models predict the tempo of speciation and can explain the patterns of diversity underlying classic radiations. In the context of these models, we have also determined the conditions necessary for mutation-induced mode of speciation; if these are not met, then fission must be the only speciation mode. Finally, we have shown that frequency-dependent selection generates more symmetric and larger incipient species abundances, resulting in lower extinction rates. These results reinforce the notion that the incipient species abundance can have a dramatic impact on contemporary diversity patterns[29], and suggest that both the tempo and mode of speciation themselves have a large effect on current community dynamics.

In summary, the particular mechanisms underlying the dynamics of the evolutionary graph affect the tempo of speciation, but we nevertheless find theoretical distributions in agreement with the observed patterns of radiations and biodiversity for diverse taxa. Underlying the result are two simple models of a sexually reproducing population with and without frequency-dependent selection and with mating restrictions that depend on genetic distance. By examining these models under different parameter combinations and confronting them with data, we conclude that although pre-existing environmental niches and geographic features may influence patterns of radiations and biodiversity, they are not necessary for their formation.

1 Methods Summary

Our simulation is a stochastic, individual-based, zero-sum birth and death model of a sexual population with overlapping generations and age-independent birth and death rates. After mating, haploid offspring differ from both parents and are produced following free recombination and mutation. According to tests of multiple model variants in the model without frequency-dependent selection, including parameter variation, sequential and synchronous mating, self-incompatibility (i.e., by adding a $q^{\max}$ to limit the reproduction of excessively similar individuals, Supplementary figure S5a), and mating and dispersal limited to adjacent patches (i.e., 8-patch Moore neighbourhood) with and without a wrapped torus (Supplementary figure S5b), our results apply quite generally, with the key required properties to generate declining through time speciation rate being the limitations on genetic distance associated with mating and the frequency-dependent selection mechanism.

1. Foote, M. The evolution of morphological diversity. *Annu. Rev. Ecol. Syst.* **28**, 129–152 (1997).

2. Rainey, P. B. & Travisano, M. Adaptive radiation in a heterogeneous environment. *Nature* **394**, 69–72 (1998).

3. Seehausen, O. African cichlid fish: a model system in adaptive radiation research. *Proc. R. Soc. B.* **273**, 1987–1998 (2006).

4. Phillimore, B., A. & Price, T. D. Density-dependent cladogenesis in birds. *PLoS Biol.* **6**, e71 (2008).

5. Klicka, J. & Zink, R. M. The importance of recent ice ages in speciation: a failed paradigm. *Science* **277**, 1666–1669 (1997).

6. Ricklefs, R. E. Estimating diversification rates from phylogenetic information. *Trends Ecol. Evol.* **22**, 601–610 (2007).

7. Alroy, J. *et al.* Phanerozoic trends in the global diversity of marine invertebrates. *Science* **321**, 97–100 (2008).

8. Newman, C. M., Cohen, J. E. & Kipnis, C. Neo-darwinian evolution implies punctuated equilibria. *Nature* **315**, 400–401 (1985).

9. Dieckmann, U. & Doebeli, M. On the origin of species by sympatric speciation. *Nature* **400**, 354–357 (1999).

10. Barrachough, T. G. & Savolainen, V. Evolutionary rates and species diversity in flowering plants. *Evolution* **55**, 677–683 (2001).

11. Gavrilets, S. & Vose, A. Dynamic patterns of adaptive radiation. *Proceedings of the National Academy of Sciences of the USA* **102**, 18040–18045 (2005).

12. Gavrilets, S. & Losos, J. B. Adaptive radiation: Contrasting theory with data. *Science* **323**, 732–737 (2009).

13. Aguiar, M. A. M., Baranger, M., Baptestini, E. M., Kaufman, L. & Bar-Yam, Y. Global patterns of speciation and diversity. *Nature* **460**, 384–387 (2009).

14. Seehausen, O. *Speciation and species richness in African cichlids* (University of Leiden, The Netherlands, 1999).

15. Grant, P. R. & Grant, R. *How and why species multiply: the radiation of Darwin's finches* (Princeton University Press, Princeton, NJ, 2008).

16. Butlin, R., Bridle, J. & Schluter, D. *Speciation and Patterns of Diversity* (Cambridge University Press, Cambridge, 2009).

17. Rosenzweig, M. L. *Species diversity in space and time* (Cambridge University Press, Cambridge, 1995).

18. Schluter, D. *The ecology of adaptive radiation* (Oxford University Press, Oxford, 2000).

19. Rosenzweig, M. L. Tempo and mode of speciation. *Science* **277**, 1622–1623 (1997).

20. Lynch, M. The frailty of adaptive hypotheses for the origins of organismal complexity. *Proceedings of the National Academy of Sciences of the USA* **104**, 8597–8604 (2007).

21. Lewontin, R. C., Kirk, D. & Crow, J. F. Selective mating, assortative mating and inbreeding: definitions and implications. *Eugenics quarterly* **15**, 141–143 (1966).

22. Kirkpatrick, M. & Ravigné, V. Speciation by natural and sexual selection: models and experiments. *The American Naturalist* **159**, S22–S35 (2002).

23. Higgs, P. G. & Derrida, B. Genetic distance and species formation in evolving populations. *Journal of Molecular Evolution* **35**, 454–465 (1992).

24. Lieberman, E., Hauert, C. & Nowak, M. A. Evolutionary dynamics on graphs. *Nature* **433**, 312–316 (2005).

25. Etienne, R. S., Alonso, D. & McKane, A. J. The zero-sum assumption in neutral biodiversity theory. *Journal of Theoretical Biology* **248**, 522–536 (2007).

26. Qvarnström, A. & Bailey, R. I. Speciation through evolution of sex-linked genes. *Heredity* **102**, 4–15 (2009).

27. Nee, S., Mooers, A. Ø. & Harvey, P. H. Tempo and mode of evolution revealed from molecular phylogenies. *Proceedings of the National Academy of Sciences of the USA* **89**, 8322–8326 (1992).

28. McPeek, M. A. The ecological dynamics of clade diversification and community assembly. *The American Naturalist* **172**, E270–E284 (2008).

29. Allen, A. P. & Savage, V. M. Setting the absolute tempo of biodiversity dynamics. *Ecology letters* **10**, 637–646 (2007).

30. Duftner, N., Koblmüller, S. & Sturmbauer, C. Evolutionary relationships of the $Limnochromini$, a tribe of benthic deepwater cichlid fish endemic to Lake Tanganyika, East Africa. *Journal of Molecular Evolution* **60**, 277–289 (2005).

2 Supplementary information

See supplementary information A1 to A3 and supplementary figures S1 to S5.

3 Acknowledgments

We thank Andrew Allen, John Alroy, Jonathan Davies, Rampal Etienne and Jai Ranganathan for useful comments and ideas on the development of the present study. CJM and SA were supported

by a Postdoctoral Fellowship at the National Center for Ecological Analysis and Synthesis, a Center funded by NSF, the University of California, Santa Barbara, and the State of California. CJM also acknowledges the support by Microsoft Research Ltd., Cambridge, United Kingdom. DA acknowledges the support of the Netherlands Organization for Scientific Research (NWO) through a VENI postdoctoral fellowship. DPV is a career researcher with CONICET, and was also partly funded by FONCYT.

4 Author Information

Correspondence and request for material should be addressed to CJM (melian@nceas.ucsb.edu).

5 Figure Legends

• **Figure 1 — Models of Evolution**. **a**, In each time step, first an individual dies. Second, parents are selected for reproduction (dotted square). Third, the dead individual is replaced by an offspring. Lastly, we recompute the species number and abundance. We then repeat the cycle. In this case the graph has two species with 5 (red circles) and 4 (blue circles) individuals. **b**, In an evolutionary graph, individuals occupy the vertices of a graph. In each time step, an individual is selected with a probability proportional to its fitness. In the model without frequency-dependent selection, individuals are selected randomly. In the frequency-dependent selection model, individuals with few connections, and therefore with more rare alleles, have more success at mating and their alleles spread quickly through the population. The process is described by a symmetric genetic similarity matrix Q, where $q^{ij} = q^{ji}$ denotes the genetic similarity between individual i and j. Dotted links represented by 0 in the Q matrix denote the similarity values $q^{ij} < q^{\min}$, indicating reproductive incompatibility.

• **Figure 2 — Radiations, number of species, and diversity (theory)**. **a**, Simulated total number of species (both extant and extinct) as a function of time for the model with (black, also used for **b** and **c**) and without frequency-dependent selection (red). Number of individuals (J = [2000]), mutation rate (μ = [10^{-3}]), and the minimum genetic similarity value ($q^{\min}$ = [0.9]), also used for **b** and **c**. Time measured in generations. After a transient phase, speciation events occur at a nearly constant rate in the model without frequency-dependent selection. In contrast, the frequency-dependent selection scenario shows a rapid series of fission speciation events followed by a plateau with very low speciation and extinctions events. **b**, Simulated number of extant species as a function of time for the model with and without frequency-dependent selection. Insets represent the species abundance distribution at stationarity. Frequency-dependent selection produces more extant species and higher diversity (inset in **b**). **c**, Simulated abundance symmetry of the new species after each speciation event. We measured the degree of symmetry in each speciation event

as $S/(S+M)$, where S and M are the size of the smallest new species and the mother species, respectively. Perfect symmetry means that the new species abundance is identical to the mother species abundance; low value means the new species abundance is much smaller than that of the mother species. Thick line represents perfect symmetry.

• **Figure 3 — Radiations, number of species, and diversity (data)**. **a**, Empirical (black circles) and predicted (red, 95% CI, Methods) species number and speciation events through time for the $Limnochromini$ cichlid tribe[30] in the Lake Barombi Mbo Lake. The best fit is given by the frequency-dependent selection model (μ = [4 x 10^{-4}], $q^{\min}$ = [0.80] and M = 8.8 (M = 9.8 for the model without frequency-dependent selection, see Methods). Inset in **a** is the relative species abundance at stationarity given by the parameter combination that best describe the data. **b**, Empirical (black circles) and predicted (red, 95%) species number and speciation events through time for the Darwin's finches[15]. The model without frequency-dependent selection has a slightly lower minimized value than the model with frequency-dependent selection (μ = [4 x 10^{-4}], $q^{\min}$ = [0.87] and M = 15.2 vs. M = 15.9 for the model with frequency-dependent selection). **Bottom**, Parameter combinations explored for the $Limnochromini$ tribe (left) and the Darwin's finches (right). Coloring indicates the likelihood value associated with different combinations of parameter values, with the region of "best fit" given by the dark blue area (Methods). The surface was plotted as log(M) for better clarity of the isoclines. Parameter combinations within the region of CI contain sequence divergence values in the range [2% - 5%] (i.e., $q^{\min}$ = [0.95,0.98]), consistent with linearized trees using DNA data[3,30].

6 Methods

For the simulations reported in the paper, we considered J haploid and hermaphroditic individuals where only one individual can exist in each site. Genomes consist of an infinite string of nucleotides and the genetic similarity between two individuals is the number of similar nucleotides along the genome. Reproduction starts with a randomly selected individual looking for a mate among all the sufficiently similar individuals. To qualify, an individual must have a genetic similarity greater than the minimum value required for fertile offspring. From all such potential mates, we select one at random. In the frequency-dependent selection model, individuals with few connections, and therefore with more rare alleles, have more success at mating and their alleles spread quickly through the population. The second individual is selected randomly among all the potential mates.

Mating produces a haploid offspring that differs from both parents following free recombination and mutation. Each nucleotide is inherited from one of the parents with the same probability. Mutation occurs with a probability μ. The results reported here are for asynchronous mating. Synchronous mating gave similar results, although speciation times were typically longer. Variations of the model without frequency-dependent selection were implemented with qualitatively similar results (Supplementary figure S5).

Results for Fig. 2 are obtained by time-averaging over 10 replicates lasting 2 x 10^3 generations each. Given J individuals in the initial population, a generation is an update of J time steps. Parameter variation does not affect the overall behaviour.

Results for Fig. 3 are obtained after 10^2 replicates for each parameter combination lasting 2 x 10^3 generations each. We sampled the transients (each generation) and the steady state at the end of each replicate (i.e., 2 x 10^3 generations) for the species through time and species abundance. We have explored 900 parameter combinations in the range $\mu \in [10^{-2},10^{-4}]$, and $q^{\min} \in$ [0.75,

0.98] that satisfy the mathematical condition required for speciation ($q^{\min} > Q^*$, Supplementary information equation A-30 and Box 1). Our results apply quite generally in a broad range of community size (Supplementary section A3 and figure S3) and speciation rates (Supplementary figure S4).

The fit to the number of species and speciation events through time was done following these steps: 1) Normalize time for observed data and each simulation from the first speciation event to present time within the range [0,1], 2) From each possible interval, starting with the size of the data until the size of the output in each simulation (2 x 10^3 generations with increments of 1 generation at each time), we generated the sequence of speciation times that minimizes the difference with the observed speciation times, and 3) Identify the best fit as the one that minimizes the sum of the absolute values of the misfits (i.e., $M = \sum_i m_i$ where $m_i = |x_i - x_{sim}| + |y_i - y_{sim}|$), where x_i, x_{sim}, y_i, y_{sim} are the empirical species richness at time i, the predicted species richness at time i, the empirical speciation event at time i and the predicted speciation event at time i, respectively. If our errors per data point are a random variable M_i following the exponential distribution, $M_i \sim exp(-m_i)$, and, assuming error independence, our measure of misfit M is the model negative log-likelihood. Confidence intervals have been calculated by taking the percentiles 0.05 and 0.95 from the distributions of values of different model replicates. Model replicates were generated with the best parameter estimates for μ and $q^{\min}$ along with a family of pairs within 2 log-likelihood units away from the minimum (Supplementary figure S4).

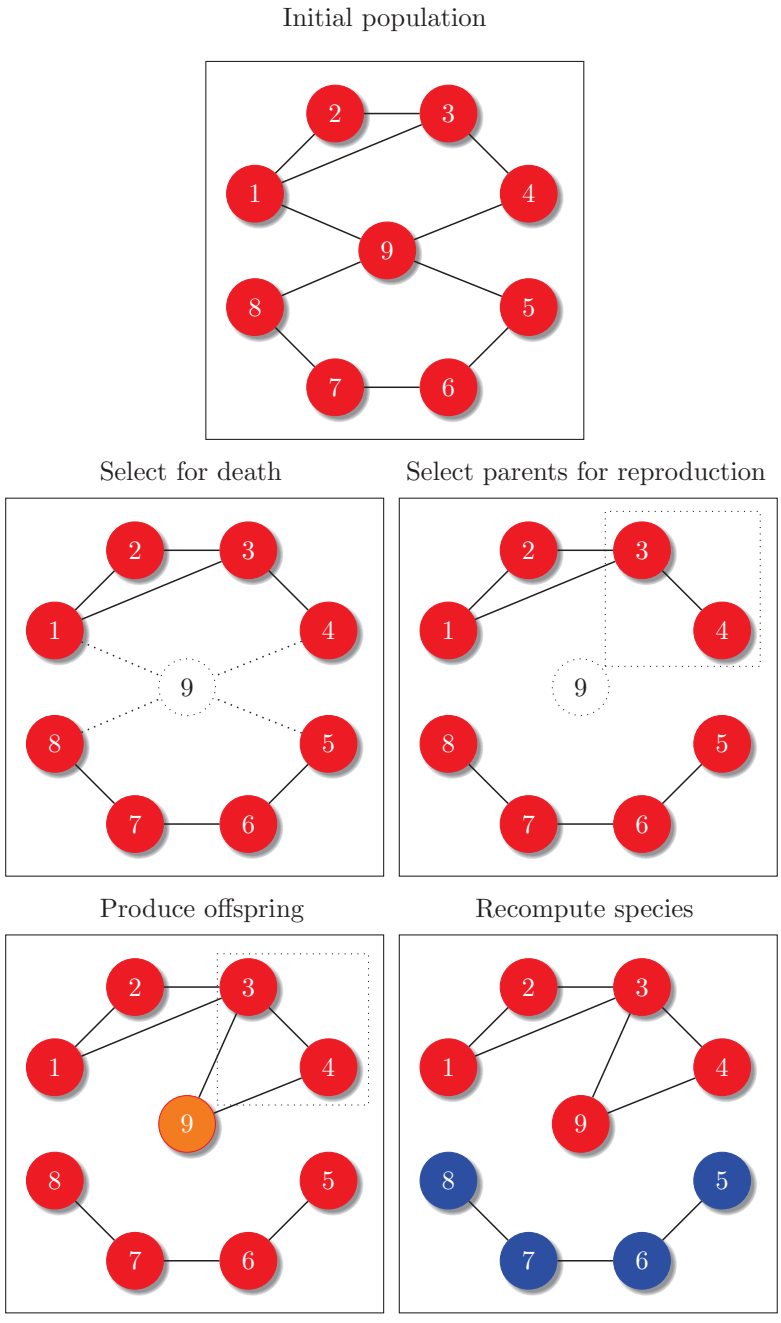
Initial population
2
3
1
4
9
8
5
7
6
Select for death
Select parents for reproduction
Produce offspring
Recompute species

Figure 1a

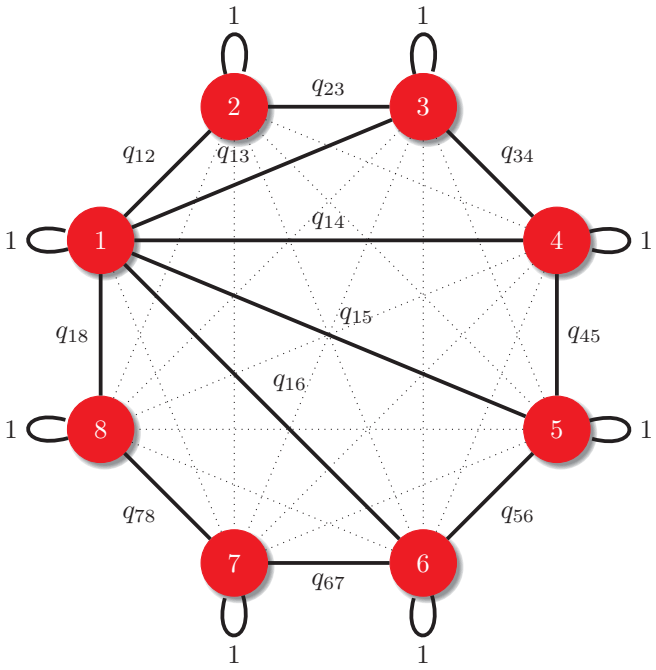

$$\mathbf{Q} = \begin{bmatrix} 1 & q_{12} & q_{13} & q_{14} & q_{15} & q_{16} & 0 & q_{18} \\ q_{21} & 1 & q_{23} & 0 & 0 & 0 & 0 & 0 \\ q_{31} & q_{32} & 1 & q_{34} & 0 & 0 & 0 & 0 \\ q_{41} & 0 & q_{43} & 1 & q_{45} & 0 & 0 & 0 \\ q_{51} & 0 & 0 & q_{54} & 1 & q_{56} & 0 & 0 \\ q_{61} & 0 & 0 & 0 & q_{65} & 1 & q_{67} & 0 \\ 0 & 0 & 0 & 0 & 0 & q_{76} & 1 & q_{78} \\ q_{81} & 0 & 0 & 0 & 0 & 0 & q_{87} & 1 \end{bmatrix}$$

Figure 1b

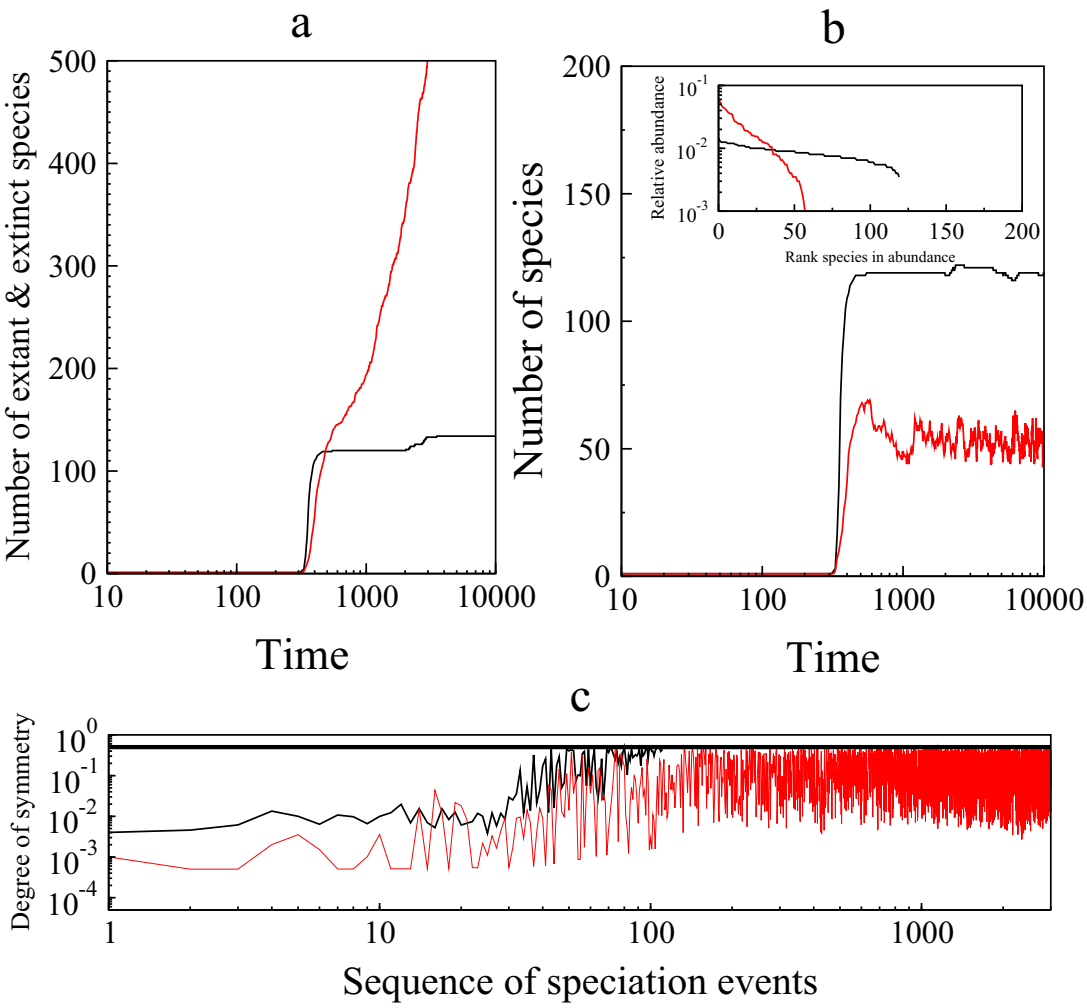
a
b
c
Number of extant & extinct species
Number of species
Time
Time
Relative abundance
Rank species in abundance
Degree of symmetry
Sequence of speciation events

Figure 2

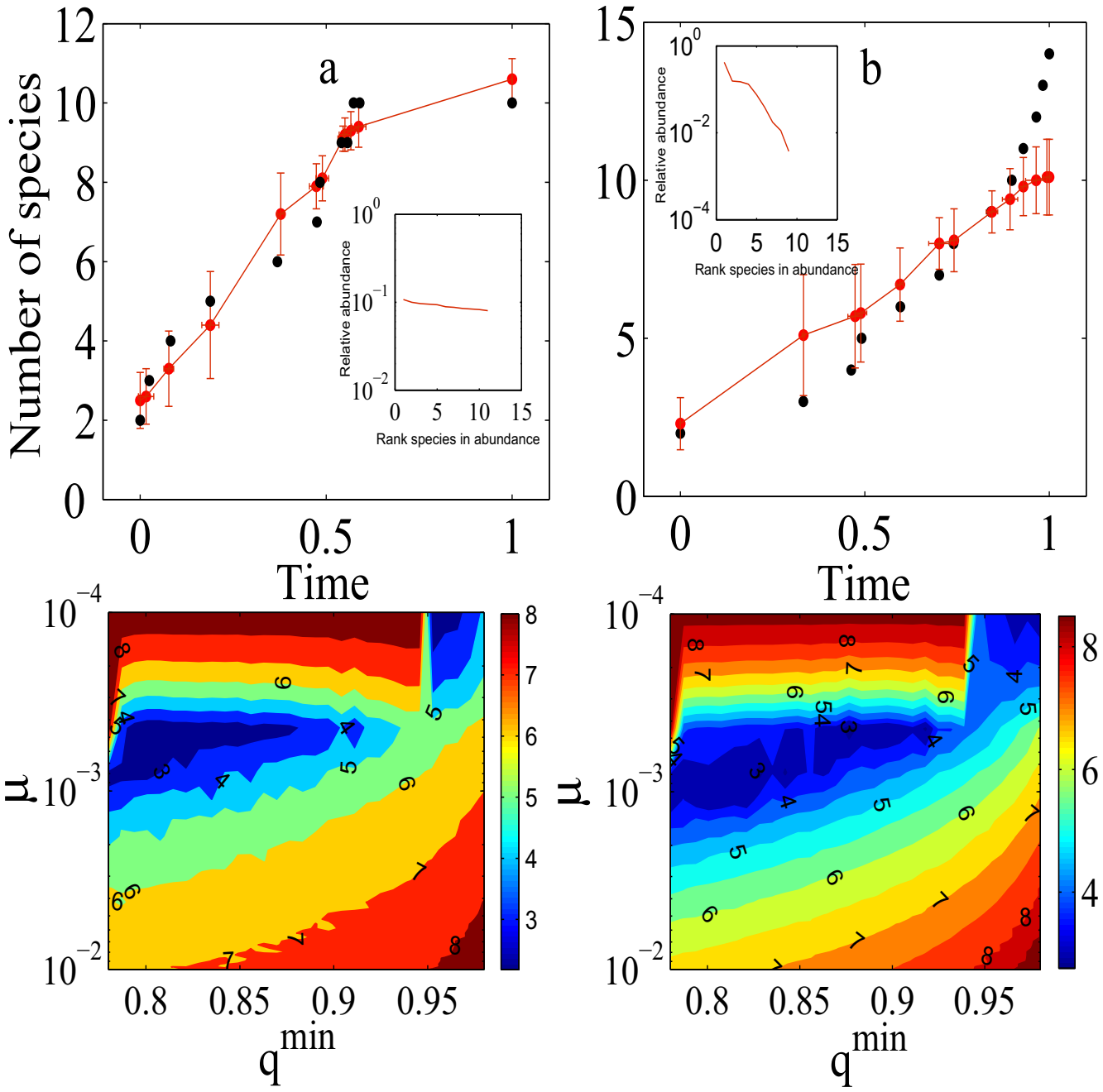
a
b
Number of species
Time
Relative abundance
Rank species in abundance
μ
q min

Figure 3